



## Applying a DOE-ACO Multi-Objective Approach toward Topology Optimization

Masoud Afrousheh<sup>1</sup>, Javad Marzbanrad<sup>1\*</sup>, Sanaz Abdollahzadeh<sup>1</sup>

<sup>1</sup>School of Automotive Engineering, Iran University of Science and Technology, Narmak, Tehran, Iran

| ARTICLE INFO   | ABSTRACT  |
|--|---|
| <p><b>Article history:</b></p> <p>Received :26 April 2019</p> <p>Accepted:28 May 2019</p> <p>Published: 01 Dec 2019</p>  | <p>Thin-walled structures play an important role in absorbing the energy in a low impact crash of vehicles up to saving lives from high impact injury. In this paper, the thin-walled columns by using a hybrid Design of Experiments (DOE) and Ant Colony Optimization (ACO) algorithm has been optimized. The analysis of the behavior of the nonlinear models under bending load is done using finite element ABAQUS software. The objective is to study the performance of geometrical parameters of the columns using DOE-ACO approach.</p>  |
| <p><b>Keywords:</b></p> <p>Ant colony algorithm</p> <p>Design of experiments</p> <p>Energy absorption</p> <p>Thin-walled column</p> <p>Topology optimization</p> | <p>DOE method is applied to determine the effects of cross-sections, material, and thickness on the energy absorption; and the ACO method is used for finding more accurate thickness on energy absorption. Four types of thin-walled cross-sections, i.e., circle, ellipse, hexagon, and square are used in this study. The optimized results of DOE method show that aluminum alloy (Al-6061) and high strength low alloy steel (HSLA) square columns have a higher energy absorption in comparison with the other cross-sections. However, the amount of absorbed energy in two types of columns is equal but, 50 percent weight reduction may be seen in Al-6061 columns. The columns are re-optimized by ACO to find the best thickness in the last step.</p> <p>In the following, by topology optimization participation, a new plan is proposed by the same thickness and 50% less weight that has a higher crashworthiness efficiency by increasing Specific Absorbed Energy (SAE) more than 70%. As a result, this plan is bridging the gap between standard topological design and multi-criteria optimization.</p> |

### 1. Introduction

In the world of Computer-Aided Design (CAD), the loudest buzz is around two technologies: generative design and topology optimization. While the generative design is a fairly recent term, the idea of topology optimization has been around for decades. Academic papers describing topology optimization stretch back to the early 1990s. Rather than generative design that seems everyone to have their own idea, topology optimization refers to a

specific algorithmic process. Topology optimization is simply a subset of generative design. Complementary to this view is the opinion that topology optimization, rather than being a subset of generative design, is an enabling technology for generative design. It's easy to see the benefits of a drastic reduction in mass. In the aerospace and automotive industries, where mass is of utmost importance, a light weighting is crucial. Indeed, these industries are among the earliest and most eager adopters of generative

\*Javad Marzbanrad  
Email Address: [marzban@iust.ac.ir](mailto:marzban@iust.ac.ir)  
<http://tlx.doi.org/10.22068/ijae.9.4.3067>

design technology. Lighter weights are important in many other applications. Fewer mass results in lower manufacturing, shipping, and material costs and may even result in a more aesthetically pleasing product.

Thin-walled columns from the perspective of protecting the vehicle occupants during collisions play an important role among vehicle parts. For energy absorption, columns are loaded in different directions, such as bending [1]. For decades, thin-walled components have been used in military and engineering industries such as automobiles and aerospace, to improve energy absorption and enhance safety [2]. The first comprehensive investigation of the performance of square and rectangular prismatic beams under bending was made experimentally and theoretically by Kecman [3]. A proposed simple failure mechanism by him involved a moving and stationary plastic hinge line. In a study on car collisions by Kallina et al. [4], are specified that more than 90% of the structural members failing was in bending collapse mode. The column members with different cross-sections are widely used in vehicles and in collisions, play a major role to absorb energy. Typically, the bending strength of the empty thin-walled columns by reaching the peak force at the small rotation declines very significantly [5]. To improve the flexural strength and weight efficiency to absorb energy, high-strength steels, and aluminum alloys are used in thin-walled structures.

A worldwide trend in the automotive industry is to develop steel grades towards higher strength while enhancing the structure in order to achieve a lightweight design [6]. Typically, the use of HSLA materials is found in parts of the cars, consist of door' side intrusion beam, Booster on B-pillar and C-pillar, Cross members and Bumper Beams [7]. Meanwhile, designing lightweight vehicles in a way that does not endanger crashworthy safety, to improve fuel efficiency and reduce the emission of toxic gases, is a vital issue. To fulfill these criteria, as of lately the application of lightweight materials such as aluminum alloys in the Spaceframe chassis has been increased [8]. For this purpose, optimization is utilized to discover adjust between economy and design execution. [9].

A study on the multi-objective optimization of hollow aluminum tubes for energy absorption in vehicle crashes is presented by Marzbanrad and Ebrahimi [10]. The optimization methods with taking a design objective and constraints that have a mathematical description functionality, present a systematic search methodology to achieve an optimum design [11]. Yamazaki and Han applied a Multi-Design Optimization (MDO) to improve the

crashworthiness properties of circular and square aluminum tubes under axial impact [12].

The metaheuristic Ant colony (AC) is an evolutionary algorithm, which has been widely employed to solve optimization problems. This strategy has been motivated by the behavior of colonies of ants when they attempt to induce nourishment. Ant algorithm originated from bionics random algorithm which is based on the natural phenomenon [13]. Research has shown that the standard Ant Colony Optimization (ACO) algorithm can be an efficient discrete optimal on-off control for the complex topology optimization problems.

In this study, the hybrid Design of Experiments (DOE) is offered to upgrade the computing performance of the standard ACO algorithm in topology optimization problems, consist of geometric nonlinearity. Multi-objective energy absorption optimization with three parameters cross-section, material, and thickness have been done. Firstly, the numerical simulation of the thin-walled column has been done through ABAQUS software. Secondly, optimization with the design of experiments is used to find the optimal cross-section and material. Thirdly, Ant algorithm optimization method to find the optimal thickness of the thin-wall column is used to absorb energy.

Due to the infirmity of the standard ACO algorithm searching the really effective elements in design lattice, and remaining the zero or negative density of elements in the stiffness matrix, gives rise to an exponential numerical instability, which leads to checkerboard problems. Given that, the optimization of the topology of nonlinear structures in comparison with linear structures requires more computational time and the standard ACO algorithm cannot give an optimized topology in geometric nonlinearity structures.

The advantage of the standard ACO algorithm is to provide a continuous variable named as "Element Contribution Significance (ECS)," which serves to move the positions of ants, according to structural response, which is derived of element' attendance, to assess the effective contribution. To prevent the formation of the checkerboard patterns in the optimization process, a mesh-independency filtering scheme is implemented [14].

According to the definition of fitness functions from papers, the pheromone value is voted as the topology's compliance which is equal to the inner product of the topology's maximum displacement ( $\delta_{max}$ ) at the point of load application. The

objective is to minimize the compliance of optimal structure [15].

The main objective of the research is to reduce the weight of the column and reduce the generated cost while energy absorption has improved. This optimized design is being constrained by the minimum strain. The column is analyzed using the finite element technique, an appropriate model of the c-pillar is to be developed. The high Specific Absorbed Energy (SAE) generated in Aluminum type column is reduced by providing a geometry of the cross-section. The numbers and levels of parameters are more; the probable models are too many. So, to select optimum parameters among them large numbers of modeling and analysis work is involved which consumes more time. To overcome this problem, the DOE technique is used along with Finite Element Analysis (FEA) [16].

In this method elimination, and restoration formula of elements imitated of ants to determine the shortest path to food [17]. Reformulating of topology optimization as a discrete problem without limitation is the main benefit of this approach. 3D examples of the models are presented to present the application of this method. Also, many of the topology optimization algorithms that have been introduced so far have been used for classical issues, such as Michell-type structures and cantilever beams with rectangular domains. So far, less attention has been paid to the application of these algorithms in 3D and real-life structures actual structures and actual loading scenarios.

## 2. Hybrid Optimization DOE-ACO

A combined method (the DOE with the ACO algorithm) has been used to minimize the range of response and to achieve a faster response. Using these two combined methods helps to find the best cross-section easily and quickly that has highest energy-absorbing. In fact, the DOE method is general searcher for columns and ACO method is to obtain the final column of thickness. The main reason for combining the two methods of optimization in the problem has been that for optimizing by an ant algorithm is required an objective function but in this study, the variables (cross-section, type of material and thickness) do not interact with each other, therefore cannot be achieved objective function that be included all three input factor. For this reason, the DOE method is used as an auxiliary tool for engineering knowledge that cross-section and material factors by which to be optimized and then, the objective function of energy absorption for ant algorithm optimization to be found according to the variable

thickness. By the ant colony one can find the unique solution.

With using the design of experiments and entering cross-sections, materials and thicknesses, a matrix of 24 on 3 which represents 24 thin-walled structure can be created which is based on the combination of these three factors. Then the output of each row of the matrix is specified. Finally, plots for the relationship between input factors and their effect on the response of output to be displayed. For this purpose, first the effect of input parameters on the output response is specified by using the main effect plot and then interaction has been checked by using an interaction point plot. Thus, the range of optimum energy absorption columns in terms of cross-section and type of material specified. At this stage observed that Columns range reduced from 24 columns to 6 columns. The following, search for the exact effects of thickness factors on the amount of energy absorption by 6 columns that ant algorithm optimization method is applied to determine the optimum thickness. For the optimization by ant colony is needed an objective function. This function in the ant colony optimization procedure as subjective information ( $\eta_{ij}$ ) is used. After finding this function, with determining the value of the initial pheromones and the pheromone evaporation rate, a program be written in MATLAB by which the optimum thickness is obtained for better energy absorption columns. In Fig. 1 Hybrid optimization DOE-ACO flowchart is shown how to solve a problem by optimizing the combination of DOE-ACO.

## 3. Design of Experiments Optimization

On this point, with the design of experiments method (DOE), more detailed factor effects on energy absorption columns were investigated. Available software in this field that the accuracy of DOE optimization is appropriate and has a quick process is Minitab. This statistical software by using determined basic factors and output request shows the optimal range of the resulting as the graph. It is also capable of determining the effect of inputs (individually and combined) on the output response. In Fig. 2 can be seen how to solve a problem with the design of experimental optimization.



**Figure 1:** Hybrid optimization DOE-ACO flowchart.

### 3.1. Factors and Responds

A total of three design variables were strategically chosen, including two shape variables, all of which are illustrated in fig. 3. Appropriate constraints were subsequently applied to the individual design variables, such as minimum (and maximum) thickness values, individual distances, etc. With the design variables specified the DOE studies could commence. The following sections will discuss the potential for employing various sampling methods for DOE, with respect to creating the aforementioned metamodel for shape and size optimization in

relation to crashworthiness and minimizing mass. Consequently, a vast number of computational permutations were required in order to complete the parameterization [18].

input factors contain cross-section, material, and thickness and the amount of absorbed energy per column is chosen as output response. This information for DOE is inserted in the form that is shown in Table 1.

## 4. Numerical Simulation

Dynamic bending crash test was carried out with the impact mass of 10.3 kg and a maximum impact speed of 10 m/s. Table 4 gives the dimensions of the hammer in the numerical simulation test and the shape of the hammer is shown in Fig. 4.

### 4.1. Material

Two types of materials are considered for thin-walled columns. The materials used for simulation are High Strength Low Alloy (HSLA) [19] and aluminum alloy (Al-6061-T6) [20] which properties are explained in Table 2 and 3.

### 4.2. Constitutive Model

The plastic behavior materials are characterized by the Johnson-Cook constitutive model, which aims to predict material behavior subjected to large strains and high strain rates such as high-velocity impacts [7]. The constitutive model is expressed as eq.1:

$$\sigma_Y = \left[ A + B(\varepsilon_{eff}^p)^N \right] (1 + C \ln \dot{\varepsilon}) \left[ 1 - \left( \frac{T - T_R}{T_M - T_R} \right)^M \right] \quad (1)$$

Where  $\sigma_Y$  is the equivalent stress,  $\varepsilon_{eff}^p$  is the effective plastic strain,  $\dot{\varepsilon}$  is the reference strain rate,  $T$  is the temperature of the specimen,  $T_M$  is the melt temperature and  $T_R$  is the reference temperature. The Johnson-Cook parameters of the materials considered in this study are listed in Table 2.

### 4.3. Formulation

The collision Absorbed Energy  $E_t$  achieved by the integration of the impact contact force (F) towards the endpoint of deflection  $U_f$  [5] (eq.2).

$$E_t = \int_0^{U_f} F du \quad (2)$$

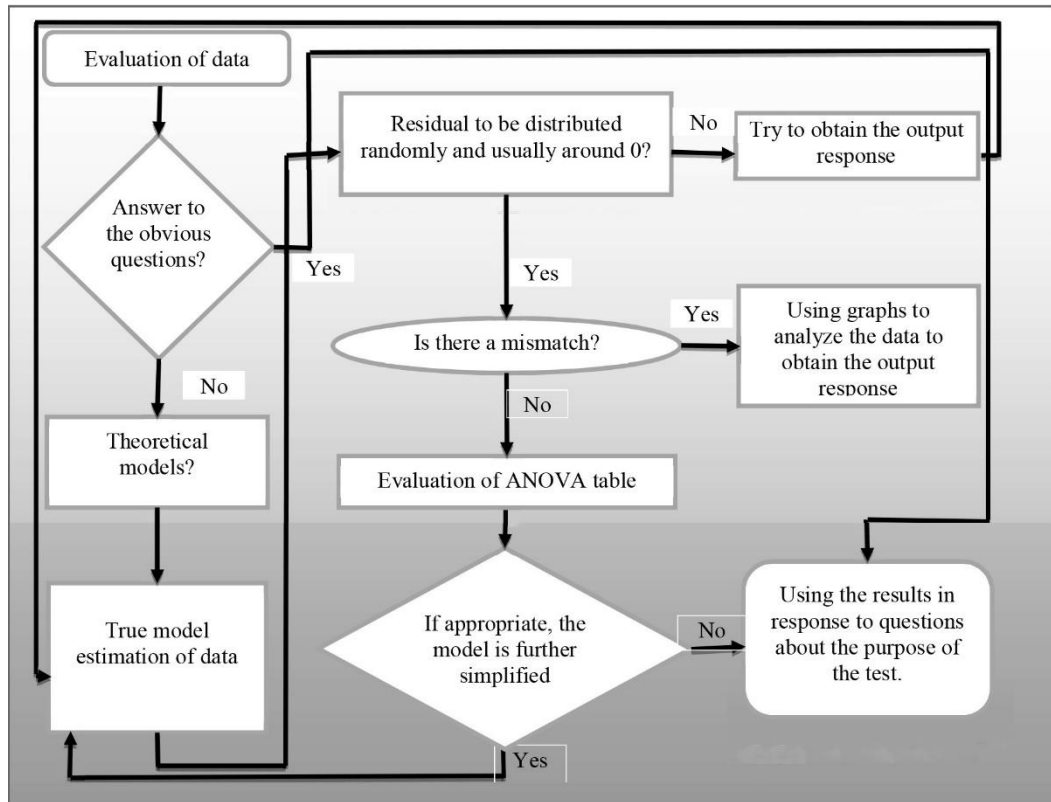


Figure 2: DOE optimization diagram.

Table 1: DOE information forms

| Factor | Name          | Type      | Levels | Level Values |         |         |        |
|--------|---------------|-----------|--------|--------------|---------|---------|--------|
| A      | Material      | Text      | 2      | AL-6061      | HSLA    |         |        |
| B      | Thickness     | Numerical | 3      | Max          | Mean    | Min     |        |
| C      | Cross-section | Text      | 4      | Circle       | Ellipse | Hexagon | Square |

Table 2: Elastic properties of materials examined

| Material | $\rho(\text{kg/m}^3)$ | $E(\text{GPa})$ | $\nu$ |
|----------|-----------------------|-----------------|-------|
| AL-6061  | 2715                  | 68.95           | 0.33  |
| HSLA     | 7842                  | 197             | 0.29  |

Table 3: Johnson-Cook parameters of examined materials

| Material | A (MPa) | B (MPa) | C    | $n'$ | $m'$ | $D_1$ | $D_2$ | $D_3$ | $D_4$ | $D_5$ |
|----------|---------|---------|------|------|------|-------|-------|-------|-------|-------|
| AL-6061  | 344     | 200t    | 0.25 | 0.33 | 1    | 0     | 4.8   | -2.7  | 0.01  | 0     |
| HSLA     | 324     | 114     | 0.02 | 0.42 | 1    | -0.77 | 1.45  | -0.47 | 0     | 1.6   |

#### 4.4. Geometry

Four types of thin-walled cross-sections, i.e., circle, ellipse, hexagon, and square are used in the numerical simulation. The cross-sections of different thin-walled columns are shown in [Fig. 3](#). The amount of energy absorption of steel thin-walled columns with three kinds of thicknesses, i.e.

1.5, 2 and 2.5 mm and aluminum thin walled columns with three-fold thicknesses, are carried out. Table 4 presented the geometry dimensions of the thin-walled columns in the numerical simulations.

**Table 3:** Dimensions of the thin-walled columns

| Cross-Section | Width (mm) | Length (mm) | Thickness <sub>AL</sub> (mm) | Thickness <sub>S</sub> (mm) | Mass <sub>AL</sub> (kg) | Mass <sub>S</sub> (kg) |
|---------------|------------|-------------|------------------------------|-----------------------------|-------------------------|------------------------|
| Circle        | 88.5       | 370         | 3                            | 2                           | 0.809                   | 01.58                  |
| Square        | 70         | 370         | 3                            | 2                           | 0.809                   | 1.58                   |
| Ellipse       | 57.5       | 370         | 3                            | 2                           | 0.809                   | 1.58                   |
| Hexagon       | 80.5       | 370         | 3                            | 2                           | 0.809                   | 1.58                   |

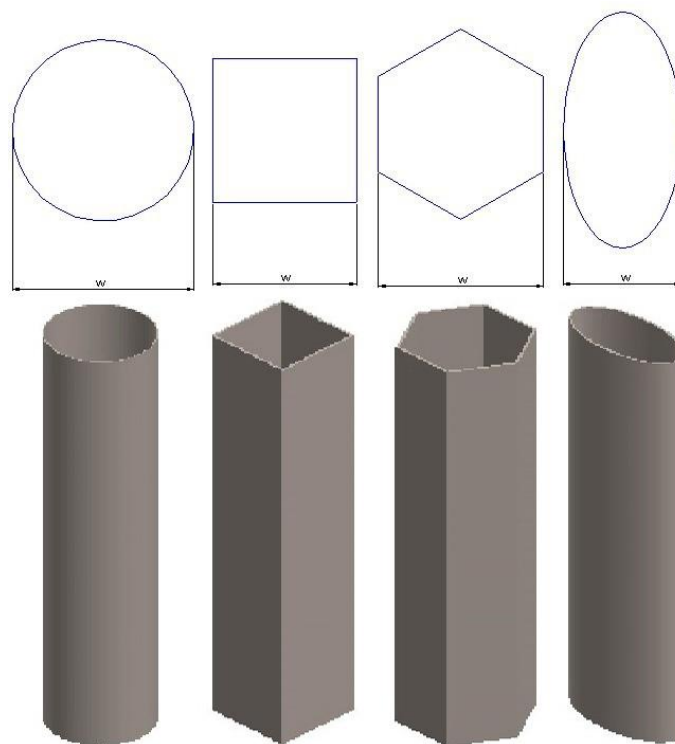


**Figure 2:** Engineering stress-strain curve at four different strain rates.

**Table 3:** Hammer parameters

| Parameters | Width (mm) | Length (mm) | Thickness (mm) | Mass (kg) |
|------------|------------|-------------|----------------|-----------|
| Hammer     | 250        | 86          | 50             | 10.3      |

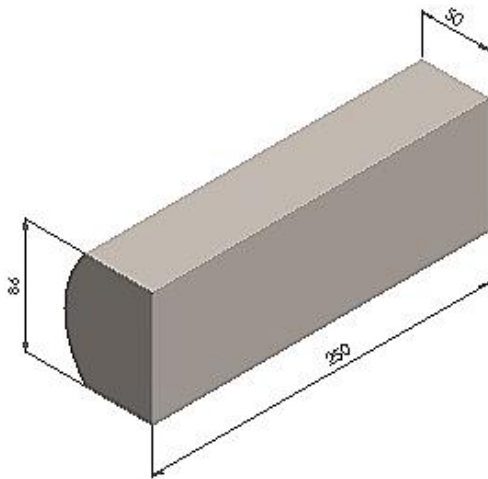


Figure 4: Hammer.

#### 4.5. Finite Element Model

For dynamic bending crash simulation, ABAQUS/Explicit software is used to determine the energy absorption behavior of the columns which are fixed in two ends and modeled as a solid structure. The finite element model of the square and hexagon columns consist of 4293 C3D8R elements and the circle and ellipse columns comprise of 4144 C3D8R elements. A three-dimensional model of a square section is shown in Fig. 5.

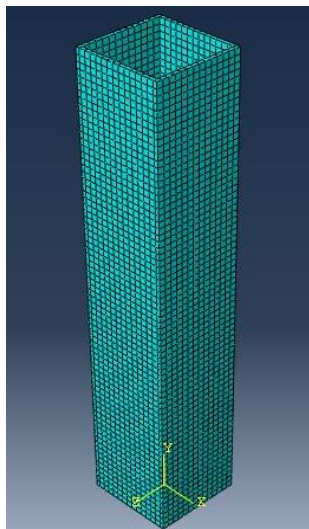


Figure 5: Three-dimensional model.

#### 4.6. Results of Simulation

The effect of the cross-section parameters on energy absorption behavior is investigated. Thickness parameter of the HSLA columns is constant ( $t=2$  mm) with  $L=370$  mm, and the speed of the impactor is  $v=10$  m/s. The load-displacement curves of different cross-sections are shown in fig. 6.

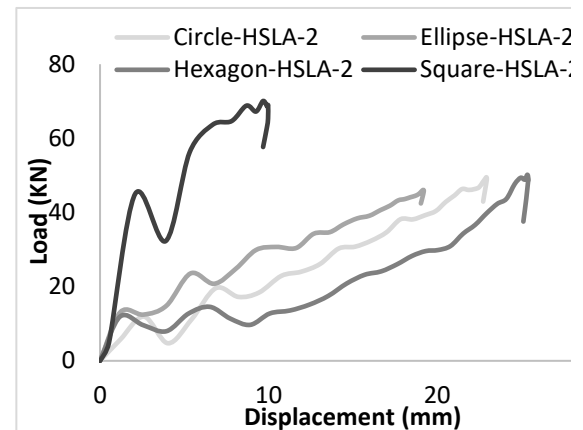
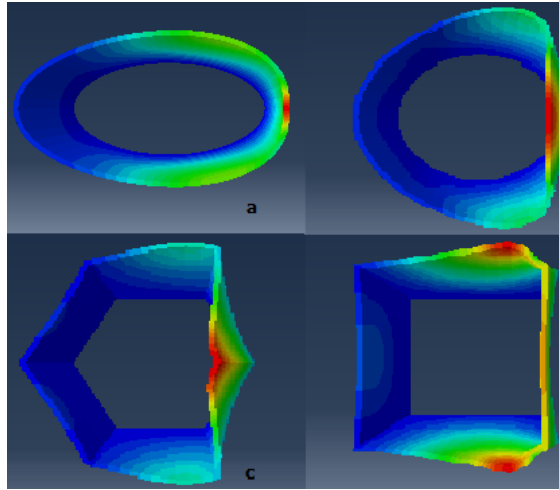


Figure 6: Load-displacement of circle, ellipse, hexagon and square steel columns.

As shown in fig. 6, the maximum area under load-displacement curves is for the square column. Then the largest amount of absorbed energy belongs to the ellipse and circular columns and hexagon column have the lowest energy absorption. Fig. 7 shows the section view of each of these deformed columns after a collision by the hammer.

After examining the cross-section, the effect of the material on the energy absorption behavior has been determined to be distinguished the difference between steel and aluminum, Al-6061. The assumed parameters for all four sections (circle, ellipse, square and hexagon) are  $t=3$  mm,  $L=370$  mm, with the speed of impactor  $v=10$  m/s. Aluminum columns are 1.5 times thicker than steel, however, the aluminum columns are about 50% lighter than steel as reported table 3.



**Figure 7:** Section view for deformation of (a) ellipse, (b) circle, (c) hexagon, (d) square columns.

It can be seen that the highest level of energy absorption is devoted to the square column. By comparison of two steel and aluminum square columns, it has been seen that the amount of energy absorption by aluminum column is 3.2% more than the steel column. Fig. 8 and 9 shown the Load-displacement curves of the two columns and section view of the deformed columns after a collision by the hammer.

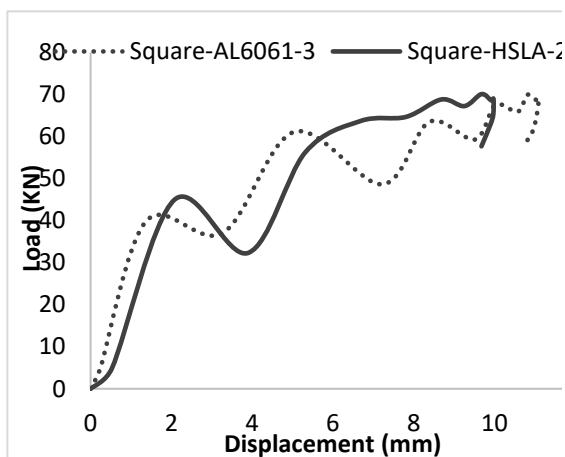


**Figure 8:** Load-displacement of steel and aluminum square columns.

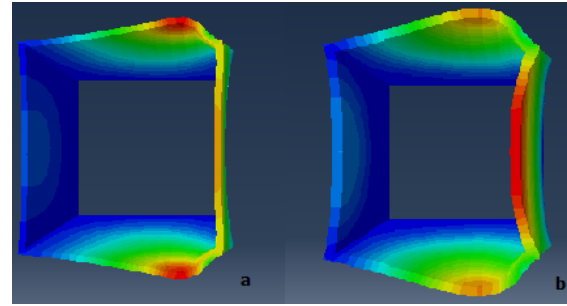


**Figure 9:** Section view for deformation of (a) steel, (b) aluminum square columns.

Another point that may be drawn is that energy absorption for aluminum hexagonal columns increases to 33.5% as compared to the steel hexagonal columns. The amount of energy absorption in the aluminum hexagonal columns after aluminum square columns and steel square columns is slightly higher than the other columns. The load-displacement curve of steel and aluminum hexagonal columns is shown in Fig. 10, while Fig. 11 shows the deformation of hexagonal columns after a collision by the hammer.

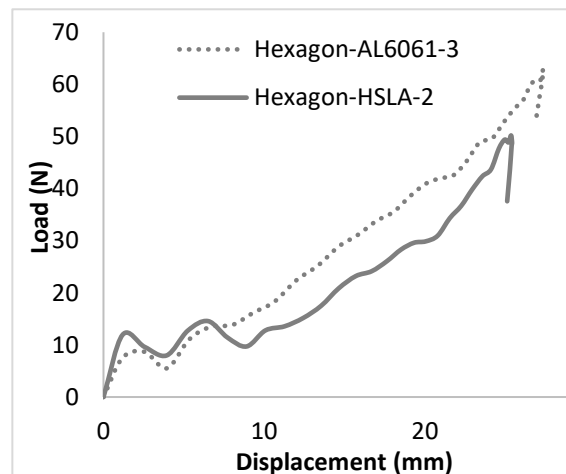


**Figure 10:** Load-displacement of steel hexagonal columns and aluminum hexagonal columns.



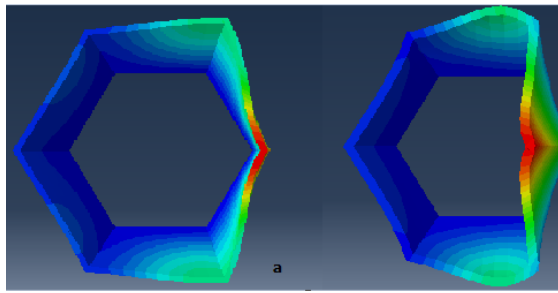


**Figure 11:** Section view of deformation (a) steel hexagonal columns, (b) aluminum hexagonal column.

Aluminum circular columns after of aluminum hexagonal columns had the maximum amount of energy absorption. After the aluminum hexagonal columns, the second largest amount of energy absorption belongs to aluminum circular columns that energy absorption has increased 13% in comparison with steel circular columns and it has increased 1.5% compared to steel elliptical columns. Fig. 12 shows Load-displacement curves of aluminum Circular columns.

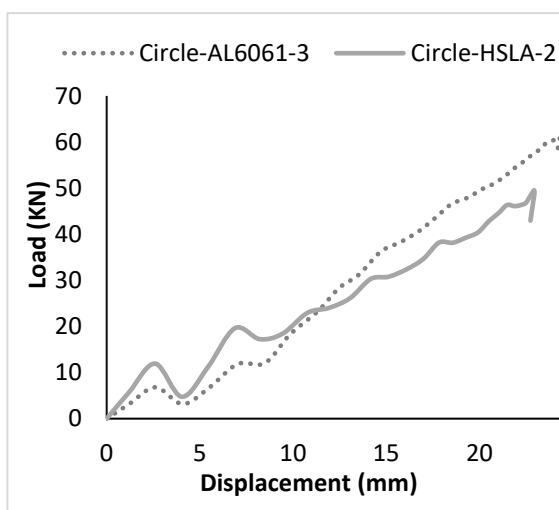


**Figure 12:** Load-displacement of steel Circular columns and aluminum Circular columns.

The elliptical column is the only cross-section that has shown lower energy absorption with the material change from steel to aluminum. Fig. 13 shows load-displacement curves of aluminum elliptical columns

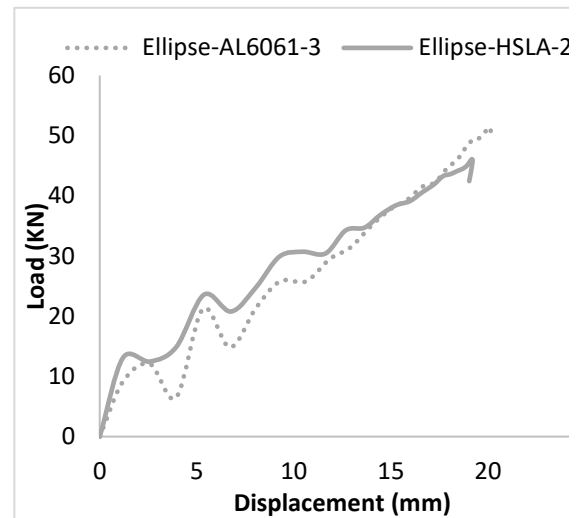


**Figure 13:** Load-displacement of steel Circular columns and aluminum Circular columns.

According to the studies that have been done in the past [21], the thickness can be a significant effect on the energy absorption behavior of thin-walled columns when subjected to a dynamic impact loading. Accordingly, the effect of thickness on the amount of energy absorption has been investigated here. The thickness of steel columns was considered 1.5~3 mm and for aluminum columns 2.25~3.75 mm. In fig 13, the load-displacement curves of 24 columns have been compared. By increasing the thickness for each section, the energy absorption rate increased for both materials. Unexpectedly, the amount of absorbed energy of hexagonal aluminum column by increasing thickness from 3 to 3.75 mm, 4% has been decreased.

As can be observed, the effect three parameters (material, thickness, and cross-section) individually was measured as the amount of energy absorption. This diagram specifies that the effect of aluminum alloy compared to the steel on the energy absorption response was greater and in overall, the aluminum columns compared to the steel columns have a higher energy absorption.

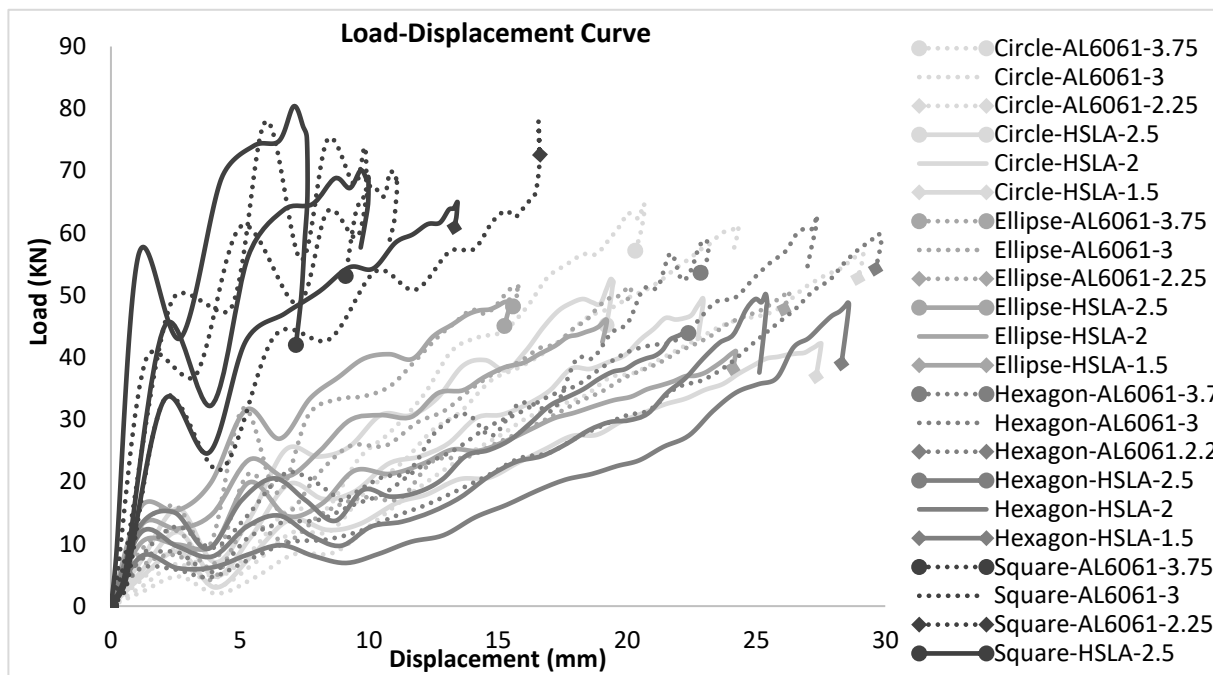


**Figure 14:** Load-displacement of steel and aluminum columns with different cross-sections and thicknesses.

Also, with increasing thickness has gone up energy absorption rate. But the slope of the plot is shown at different points that thickness range is considered for aluminum and steel columns of the minimum thickness to moderate has energy absorption more than the moderate thickness to high. In other words, by reducing the thickness, the rate of decline energy absorption has increased but the greater thickness of moderate to high, the rate of energy absorption has increased much less. Similarly, in the cross-section can be seen that square cross-sections have a high effect on the energy absorption compared to three other cross-sections and so it to respectively, elliptical, circular and hexagonal cross-section have been effective. In the next step, fig 15 shows the interaction of factors on each other and in this way, the effect of input factors on the output response has been measured two by two.

In the first part of the plot, the effect of material parameters and thickness has been measured on the energy absorption. It has been observed that by changing the thickness of 3 mm to 2.25 mm, the amount of effect on the

energy absorption for aluminum columns has been higher and energy absorption has been greatly reduced. But with increasing thickness of 3 mm to 3/75 mm, slightly has increased energy absorption. Rat of energy absorption for steel columns the increasing trend has been fixed by changing the thickness of 1.5 mm to 2 mm and from 2 mm to 2.5 mm.

In the second part of the plot, the effect of material parameters and cross-section has been measured on the energy absorption. For aluminum materials, the effectiveness of three cross-sections, circle, ellipse and hexagon on the energy absorption has been alike, but aluminum square cross-sections have higher energy absorption levels. Respectively for steel columns, hexagon, circle, and ellipse cross-sections the effect of steady have increased on the energy absorption. Among these, square steel columns had the highest rate of energy absorption that this rate has slightly higher than the aluminum square columns.

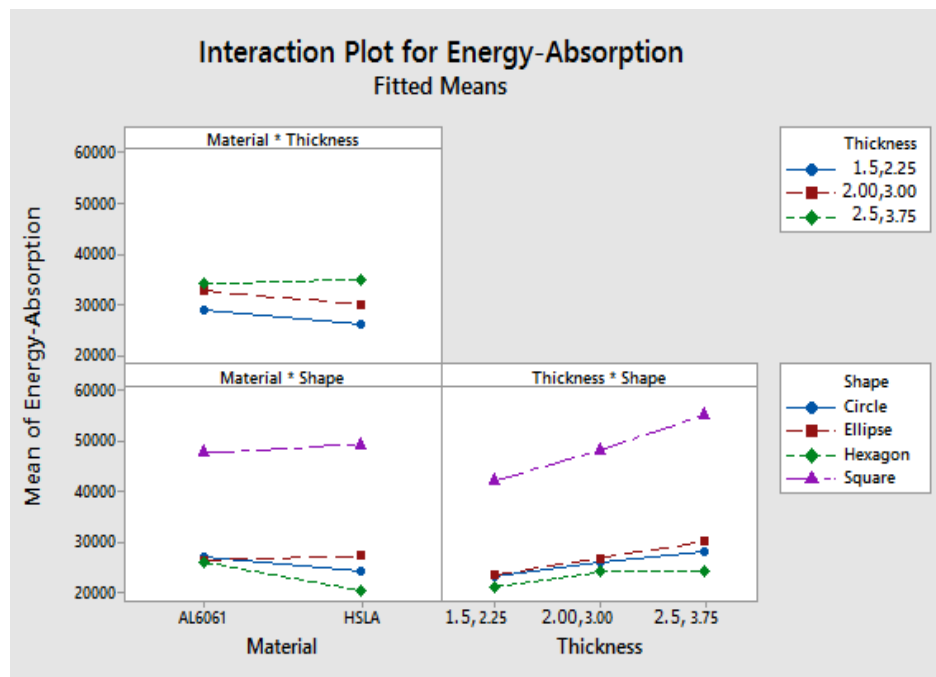


**Figure 14:** Interaction plot for energy absorption.

In the third part of the plot, the effect of cross-sections parameters and thickness on the energy absorption has been measured. Hexagon columns with different thicknesses had the least amount of energy absorbed. In these columns, energy absorption has been increased with increasing thickness up to the average value of the range but the diagram shows that energy absorption decreased with increasing thickness of the medium to high. In the circular cross-sections has been absorbed more energy from the hexagon cross-sections and energy absorption trend is constant by increasing the thickness of circular cross-sections as shown in fig. 15. The elliptical cross-sections more energy has absorbed of the two cross-sections circular and hexagonal and also with increasing thickness, the elliptical columns has been fixed energy absorption. Recent cross-section evaluated is square cross-sections. This cross-section had the highest rate of energy absorption and according to the slope from the plot with the increase in thickness has a strong upward trend in the energy absorption.

To assess the validity of analysis is used the normal curve. Fig. 16 shows the normal probability plot. If the plot is a line approximately straight, analysis carried out is validated and otherwise, the result is not valid. In this diagram, the location of the points are around the straight line which indicates the accuracy of the result.

Each point on the plot represents one of the 24 columns. And the percentage of each of them is shown on the energy absorption. The upper right corner is the point of the square columns.

In the last step, by using DOE optimization can be found more or less, and even specific amount of output (among a large number of tests). For example, in this study, the steel square columns with a thickness of 2.5 mm by specifying the maximum amount of energy absorption has been introduced as a function, that can be seen in fig. 17.



Figure 16: Normal probability plot.

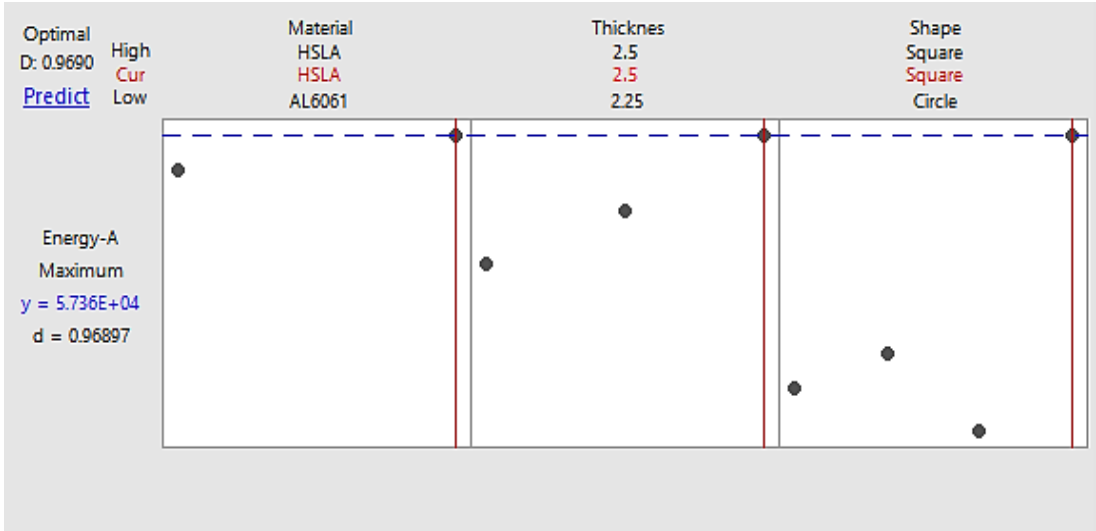


Figure 17: Plot optimization.

#### 4.7. Result of DOE Optimization

According to the plots, square columns are the best energy absorbing. Also, with increasing thickness in these columns, energy absorption has been increased regularly. But it is significant for both steel and aluminum materials because energy absorption difference is small. Cross section-material line slop in Fig. 15 is very low and this line is almost as horizontally. It is representing that the energy absorption is equal to both materials in this type of columns. On the other hand, the aluminum columns weight is less compared to steel columns. The conclusion is that a range of 24 different columns based on the results obtained from the design of experiments is limited to the 6 square columns of steel and aluminum. Design of experiments has shown that square columns are optimized for the cross-section and both materials are suitable but if we want to consider the lightweight vehicles should be selected aluminum square columns as the final column.

#### 5. Ant Colony Algorithm

In following, by considering thickness factors and its effect on the energy absorption, optimization of the aluminum and steel square columns with ACO by foraging behavior of ants have been investigated [22]. Fig. 18 shows the ACO algorithm.

##### 5.1. Objective Function in ACO

In this study, the absorption energy is chosen as an objective function. To find this, table 6 is provided for aluminum and steel square columns, which reported according to energy absorption and weight changes by considering thickness changes.

According to the given values, fig 19 shows the thickness-energy absorption curves for both types of aluminum and steel column.

**Table 6:** Energy absorption with considering the changes in the thickness

| Column              | Thickness (mm) | Mass (kg) | Energy absorption (J) |
|---------------------|----------------|-----------|-----------------------|
| Square-HSLA-1       | 1              | 0.801     | 34418.02              |
| Square-HSLA-1.25    | 1.25           | 0.997     | 37676.66              |
| Square-HSLA-1.5     | 1.5            | 1.193     | 42240.18              |
| Square-HSLA-1.75    | 1.75           | 1.39      | 45200.93              |
| Square-HSLA-2       | 2              | 1.58      | 47520.25              |
| Square-HSLA-2.25    | 2.25           | 1.77      | 50060.72              |
| Square-HSLA-2.5     | 2.5            | 1.96      | 58610.57              |
| Square-HSLA-2.75    | 2.75           | 2.15      | 63036.3               |
| Square-HSLA-3       | 3              | 2.33      | 66382.73              |
| Square-AL6061-1.5   | 1.5            | 0.413     | 34354.25065           |
| Square-AL6061-1.875 | 1.875          | 0.513     | 36708.67012           |
| Square-AL6061-2.25  | 2.25           | 0.613     | 42248.92028           |
| Square-AL6061-2.625 | 2.625          | 0.711     | 44723.93995           |
| Square-AL6061-3     | 3              | 0.809     | 49077.57101           |
| Square-AL6061-3.375 | 3.375          | 0.904     | 50491.37265           |
| Square-AL6061-3.75  | 3.75           | 0.998     | 52010.74666           |
| Square-AL6061-4.125 | 4.125          | 1.09      | 58124.23145           |
| Square-AL6061-4.5   | 4.5            | 1.18      | 59314.77882           |

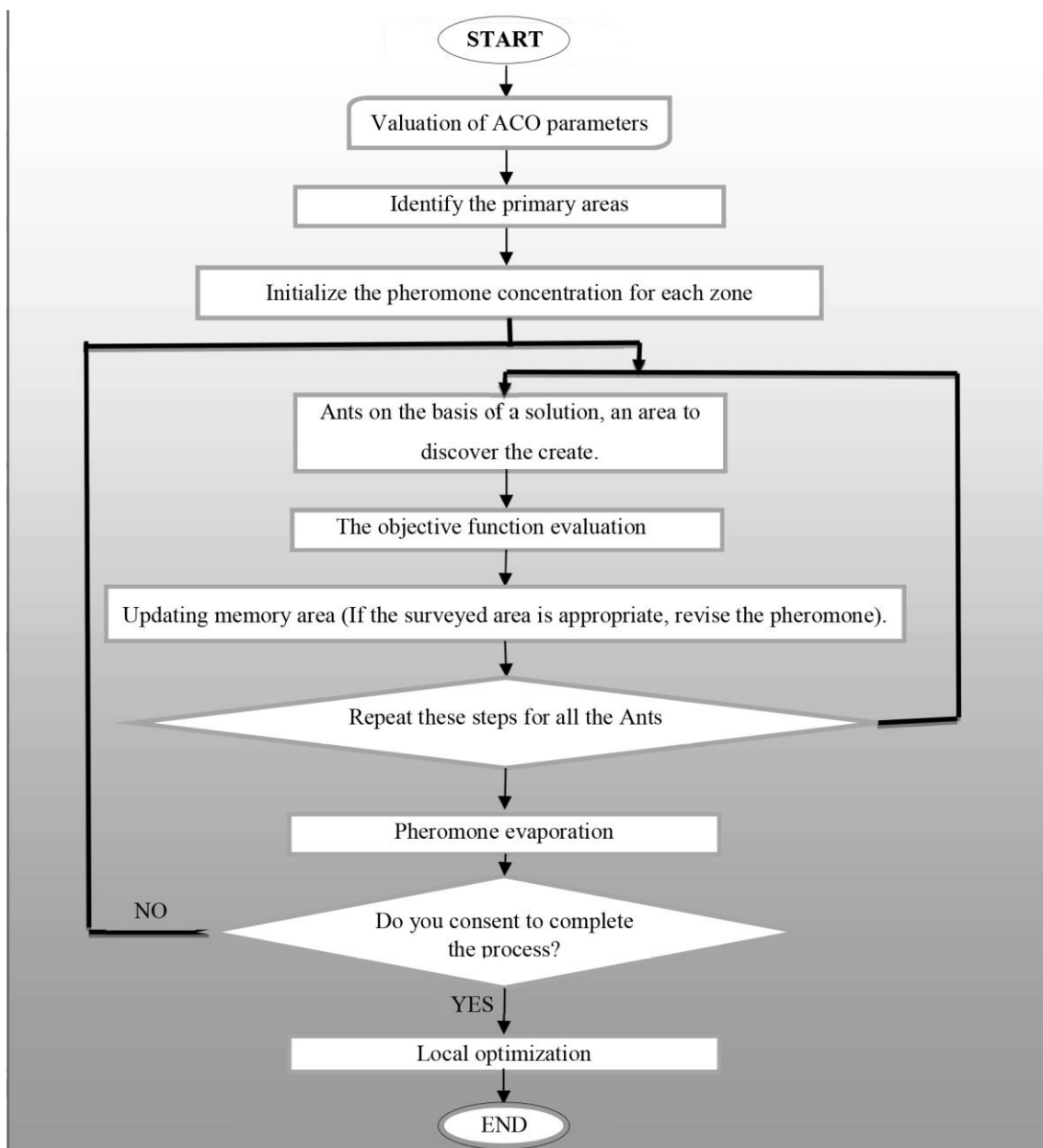


**Figure 18:** Ant algorithm flowchart.

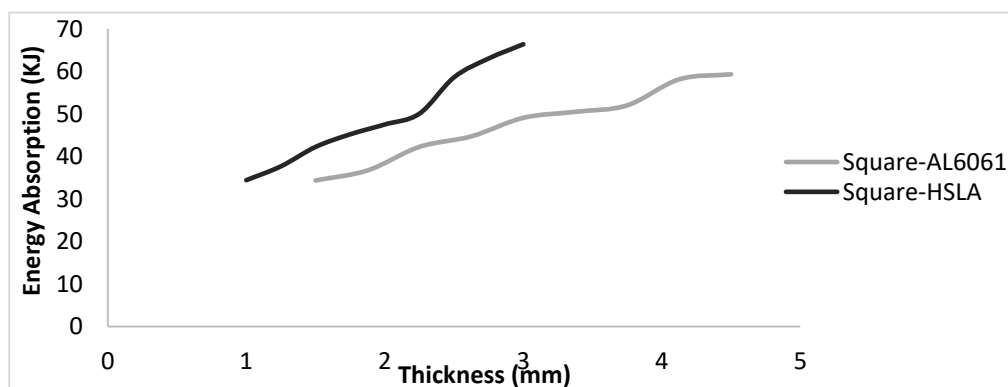


**Figure 19:** Energy absorption for different thickness of square sections.

In figure 19, it can be seen that neither of thickness, energy absorption curves of steel nor aluminum columns is not a straight line. Therefore, the objective function has been found for both steel and aluminum square columns by using the values of the thickness and energy absorption and writing a program in the MATLAB software. This Fourier series can determine the amount of energy absorption by the thickness. The required equations are described below (eq (3) and (4)).

$$f(x) \approx \frac{a_0}{2} + \sum_{n=1}^{\infty} \left( a_n \cos \frac{n\pi}{L} x + b_n \sin \frac{n\pi}{L} L \right) \quad (3)$$

$$\begin{aligned} a_0 &= \frac{1}{L} \int_{-L}^{+L} f(x) dx \\ a_n &= \frac{1}{L} \int_{-L}^{+L} f(x) \cos \frac{n\pi}{L} x dx \\ b_n &= \frac{1}{L} \int_{-L}^{+L} f(x) \sin \frac{n\pi}{L} x dx \end{aligned} \quad (4)$$

Thickness ranges are  $1 \leq t \leq 3$  for steel columns and  $1.5 \leq t \leq 4.75$  for aluminum columns. Function  $f(x)$  is taken considered as a straight line between the colons of thickness.

## 5.2. ACO Algorithm

In the optimizing of the ant algorithm,  $n$  points should be taken as the number of columns with different thicknesses that are named vertex. In this case, 9 vertexes are considered for each of the aluminum and steel square columns, where the height of vertices are representing the amount of energy absorption. In the second step, a matrix with one row and  $n$  columns as vertices number are formed. In the following, a number of artificial ants are on the case and according to a certain probability, choose the next destination for their movement. For this work, pheromone and subjective information are necessary.  $\tau_{ij}$  is the

initial pheromone that in the first stage, an amount is equal to be put in all directions and in the next step, this value will be changed by the ants.  $\eta_{ij}$  is the pheromone that according to the amount of energy absorption (the height of vertex), each ant to leave behind when the passing of each vertex and this amount is equal to the same objective function. The possibility of an ant moves from a vertex to another vertex may be illustrated via the following equation:

$$p_{i \rightarrow j}^k = p_{ij}^k = \begin{cases} \frac{(\tau_{ij})^\alpha (\eta_{ij})^\beta}{\sum_{m \in N_i^k} (\tau_{im})^\alpha (\eta_{im})^\beta}, & j \in N_i^k \\ 0 & N_i^k \end{cases} \quad (5)$$

$\alpha$  is the amount of influence  $\tau_{ij}$  and  $\beta$  is the amount of influence  $\eta_{ij}$ . In this study,  $\alpha$  and  $\beta$  have been considered 1 and 2, respectively. Meanwhile, some amount of pheromone is evaporated as below (eq (6)):

$$\tau_{ij}(t) \leftarrow (1 - \rho) \tau_{ij}(t), \rho \in (0, 1] \quad (6)$$

where  $\rho$  is the evaporation rate.

Evaporation rate has a direct effect on the convergence of the algorithm. In this study,  $\rho$  have been considered 1.

## 5.3. ACO Algorithm

After determining all data, the optimal thickness has been found for both types of steel and aluminum square columns with the aim of more energy absorption. It can be seen that the highest energy absorption obtained of steel square columns with 2.9 mm thickness and aluminum square columns with 4.3 mm thickness.

An ant colony method like a Genetic algorithm is classified as a stochastic method. Although computing in the stochastic methods in comparison with the standard deterministic ones is more costly, but it performs better in a confrontation of problems with a nonlinear function (both objective function and constraints) and a large number of local extrema [23]. Many of these problems can be

troubleshooting by addressing to use of topology optimization.

## 6. Hybrid Topology Optimization

The complexity of the optimization problem because of technical constraints and various design objectives has led to the use of an intelligent design algorithm in order to obtain a quality solution in a reasonable time. Subsequently, analysis resort to utilize iterative optimization algorithms which have demonstrated to be effective in ideally tackling a tremendous assortment of nonlinear problems in different disciplines. The problem can be formulated as below:

$$\begin{aligned} \min_{\rho} \quad & F = F(\mathbf{u}(\rho), \rho) = \int_{\Omega} f(\mathbf{u}(\rho), \rho) dV \\ \text{s.t} \quad & G_0(\rho) = \int_{\Omega} \rho dV - V_0 \leq 0 \\ & G_j(\mathbf{u}(\rho), \rho) \leq 0 \quad \text{with } j = 1, \dots, m \end{aligned} \quad (7)$$

The formula variables are defined as:

- A fitness function  $F(\mathbf{u}(\rho), \rho)$ , Generally, these type of problems are defined with the goal of minimizing compliance to achieve the best performance of the structure [24].
- A design variable is a material distribution that is described by the density of material at each location  $\mathbf{u}(\rho)$ , determined by a 1 indicate a presence of materials or 0 is a sign of a cavity.
- The design space  $\Omega$ . This indicates the initial lattice domain, which is constrained by special boundary conditions.
- $m$  constraints.  $G_j(\mathbf{u}(\rho), \rho) \leq 0$  a characteristic that the solution must satisfy. Examples are the maximum amount of material to be distributed (volume constraint) or maximum stress values.

The Modified Hybrid Cellular Automata (MHCA) algorithm has recently been proposed, which shows that the efficiency of these algorithms can be improved with new

definitions [25]. One heading of inquiring about taken by analysts in this issue is the hybridization of ACO with other methods. The target for hybridization is to progress the exploration or exploitation (or both) capabilities of given methods. Exploration is concerned with looking a wider range of the solution space whereas exploitation centers on intensifying the local search. As far as ACO is concerned, hybridization endeavors have been made to move forward exploration or exploitation capabilities of the methods [26].

Topology optimization provides a stable and robust topology for geometrically nonlinear structures [27]. In this paper, a modern calculation based on the ACO-DOE approach is proposed in topology optimization for geometrically nonlinear problems. The topology optimization design basis is based on the uniform distribution of plastic strain by minimizing an objective function and avoids than stress concentration in the model. In this method, the elements that have a very small density removed, and the elements having a very large density are powered by its neighbors.

The design domain, which should be classified into finite elements, is a rectangular profile with a length of the designed columns with a cross-sectional shape in which all four cross-sectional models fit into this model. The initial domain for topology optimization is shown in fig 20.

Initial design domain consists of 553,520 elements. Since the aluminum columns have better results, just aluminum material is considered for topology optimization was done by considering two casting and extrusion constraints. The results of these optimized model are shown in fig 21. The optimization continues until the optimized model decreases the weight of the considered columns. The thickness of the optimized models is the same as the base columns (3 mm).



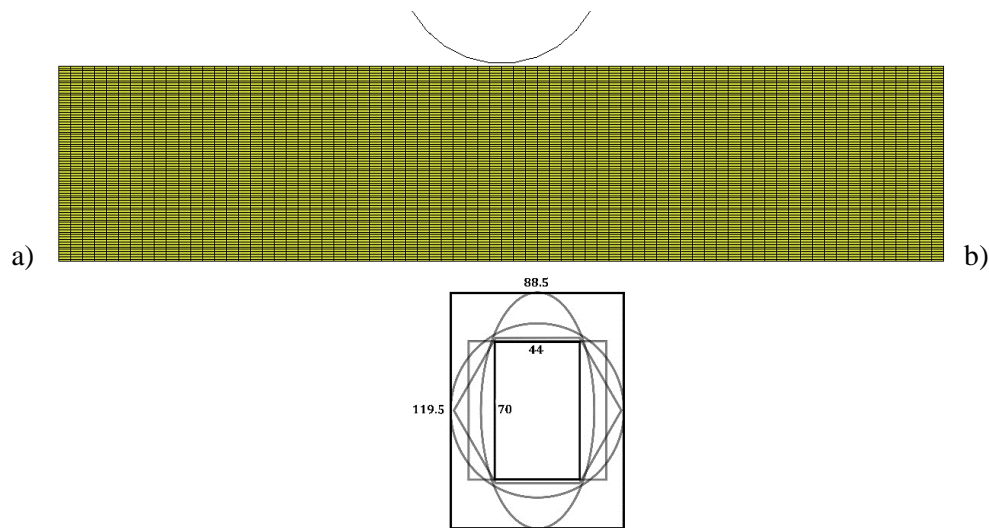


**Figure 20:** Initial design domain. a) Rectangular hollow section is discretized with  $1\text{mm} \times 1\text{mm} \times 5\text{mm}$  elements, b) Cross section dimensions.

For topology design, two manufacturing capability constraints are also considered. In addition to considering the weight of the considered columns as the objective function of topology optimization, it has also been attempted that thickness of the optimized column reach to the thickness of the initial columns, to determine the effect of topology optimization on the cross-sectional shape of the designed column than others. Firstly, due to select a mass fraction=11%, then by considering a casting constraint, an optimized model as shown in fig 21, is designed. This model has 6% less weight (58,164 elements) than Square-AL6061-3. Maximum thickness is 3mm and the minimum thickness is 2mm. the maximum plastic strain is 8.88. Maximum deflection 9.6mm that is reduced by 13.5% compare to deflection of (11.1 mm).

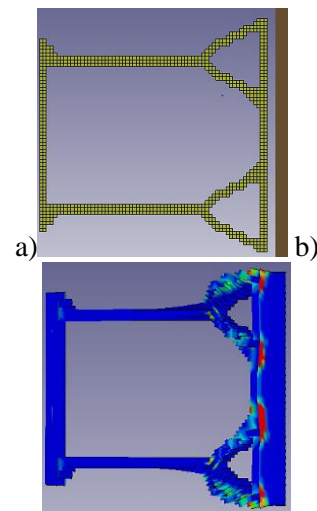


**Figure 21:** Section view of (a) optimized model by casting constraint, (b) deformation of the model.

By selecting a thickness (3mm) as an objective function and choosing an extrusion constraint, the optimized model as shown in fig 22 is designed. This model has 50% less weight (36,038 elements) in comparison to Square-AL6061-3 model (62,160 elements), also absorbed energy increased 2.3%, so SAE increased 76.46%. In the following, the load-

displacement curve of these optimized model by different constraints is compared in fig 23.

As shown in fig 23, in addition of controlling a peak load of crushing, in casting model, the contact force is decreased completely and by a progressive crushing, the kinetic energy of the hammer is absorbed as plastic deformation, while the deflection of the bottom of the column is zero.

### 7. Conclusions

In this paper, the energy absorption capacity of the thin-walled columns is investigated. For the sake of the more detailed evaluation, the circular, elliptic, hexagonal and square cross-sectional columns with various thicknesses for the HSLA and Al-6061 materials are simulated and analyzed. After that, multi-objective optimization is investigated using Hybrid DOE-ACO. In the following, by topology optimization, the new geometry of cross-section with better crashworthiness efficiency is determined.

The Ant Colony Optimization as one of the heuristic methods is applied in this research. Generative design techniques use the computer as a designer to create shapes that would be impossible for a human engineer to devise.



**Figure 22:** Section view of (a) optimized model by extrusion constraint, (b) deformation of the model (c) Cross section dimensions.

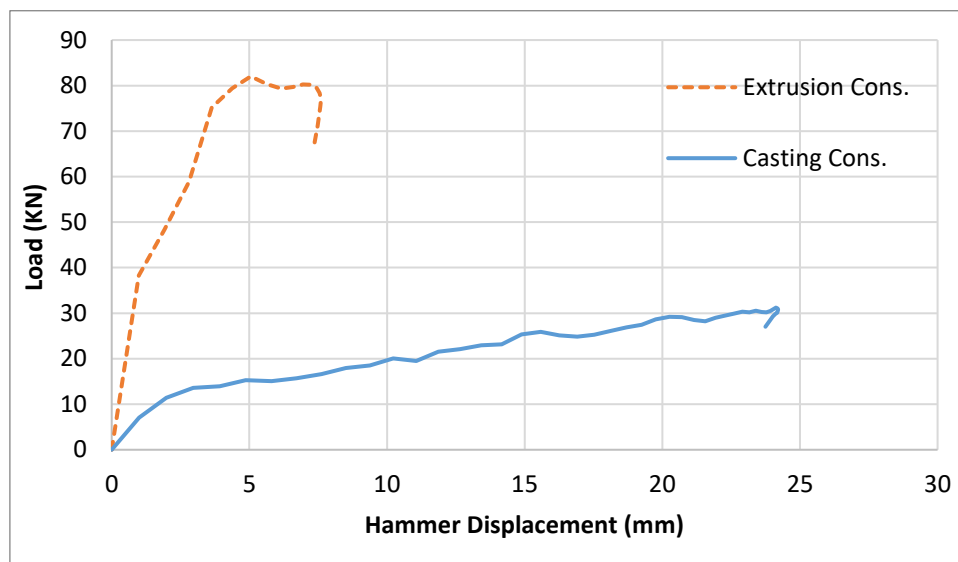


**Figure 23:** Comparison of Load-Displacement curve of an optimized model by different constraints (casting and extrusion).

Generative design techniques, especially topology optimization, have only recently achieved real practicality. Though these

techniques have been studied for decades, the results of topology optimization have been impractical to manufacture. Optimization of

cross-section and type of material is derived by using the optimization design of experiments. Then, the optimization of thickness is studied by using the ant algorithm.

The optimization problems with a huge number of design variables, which is the case in structural topology optimization, well able to be handled by Ant algorithm. In some cases, the resulted formats by ACO are not exceptionally impressive and also symmetrically. Surprisingly, when it is utilized together with a DOE method and topology optimization, very great quality formats are gotten.

According to this research on cases with different pheromone definitions, the proposed algorithm can solve the multi-objective and topology optimization of structure effectively and viable. From the results, the following achievements are summarized:

- (i) According to simulated results, energy absorption of the column is made of aluminum is more than steel column. Also, the weight of aluminum columns with different thickness is about 50% less than steel columns.
- (ii) A thin-walled square cross-sectional column has more energy absorption than that of the circular, elliptical and hexagonal cross-sectional column. Crashworthiness efficiency in the topology optimized model that is combined of the square and circular cross-section, is much higher.
- (iii) According to the results of ant colony optimization and DOE design, the best thickness for the aluminum square column is 2.9 mm and for the steel square column is 4.3 mm.

The calculation created in this research, because of the limited number of variables and single objective function, is easy to be trapped into local optimum. So, within the future, there ought to be a stronger instrument to solve this problem, such as developed multimodal and multi-objective optimization, and parallel processing to advance the capacity of adjusted ACO algorithm in solving other complex real-life engineering optimization issues.

## References

- [1] Y. Liu, M.L. Day. "Bending collapse of thin-walled circular tubes and computational application." *Thin-Walled Structures* 46, no. 4 (2008), pp.442-450.
- [2] G. Manikandaraja, "Numerical study on energy absorbing characteristics of thin-walled tube under axial and oblique impact." *Alexandria Engineering Journal* 55, no. 1 (2016), pp.187-192.
- [3] D. Kecman, "Bending collapse of rectangular and square section tubes." *International Journal of Mechanical Sciences* 25, no. 9-10 (1983), pp.623-636.
- [4] I. Kallina, F. Zeidler, K.H. Baumann, D. Scheunert. "The offset crash against a deformable barrier, a more realistic frontal impact." In *Proceedings: 14th International Technical Conference on the Enhanced Safety of Vehicles, National Highway Traffic Safety Administration, Washington, DC. (1995), pp.1300-1304.*
- [5] L. Guo, J. Yu. "Dynamic bending response of double cylindrical tubes filled with aluminum foam." *International journal of impact engineering* 38, no. 2-3 (2011), pp.85-94.
- [6] S. Stoycheva, D. Marchese, C. Paul, S. Padoan, A.S. Juhmani, I. Linkov. "Multi-criteria decision analysis framework for sustainable manufacturing in automotive industry." *Journal of Cleaner Production* 187 (2018), pp.257-272.
- [7] P. Oscar, R.L. Eduardo. "Impact performance of advanced high strength steel thin-walled columns." In *Proceedings of the world congress on engineering, vol. 2, London U.K. (2008), pp.2-4.*
- [8] A. Deb, M.S. Mahendrakumar, C. Chavan, J. Karve, D. Blankenburg, S. Storen. "Design of an aluminium-based vehicle platform for front impact safety." *International journal of impact engineering* 30, no. 8-9 (2004), pp.1055-1079.

- [9] G. Bekdaş, "Harmony search algorithm approach for optimum design of post-tensioned axially symmetric cylindrical reinforced concrete walls." *Journal of Optimization Theory and Applications* 164, no. 1 (2015), pp.342-358.
- [10] J. Marzbanrad, M.R. Ebrahimi. "Multi-objective optimization of aluminum hollow tubes for vehicle crash energy absorption using a genetic algorithm and neural networks." *Thin-Walled Structures* 49, no. 12 (2011), pp.1605-1615.
- [11] H.R. Zarei, M. Kröger. "Multiobjective crashworthiness optimization of circular aluminum tubes." *Thin-walled structures* 44, no. 3 (2006), pp.301-308.
- [12] K. Yamazaki, J. Han. "Maximization of the crushing energy absorption of tubes." *Structural optimization* 16, no. 1 (1998), pp.37-46.
- [13] A. Colomi, N. Dorigo, V. Maniezzo, "Distributed optimization by Ant Colony". In: *Proceedings of the First European Conference on Artificial Life*. USA. (1991), pp.134-142.
- [14] K.S. Yoo, S.Y. Han. "A modified ant colony optimization algorithm for dynamic topology optimization." *Computers & Structures* 123 (2013), pp.68-78.
- [15] Ch.Y. Wu, Ch.B. Zhang, Ch.J. Wang. "Topology optimization of structures using ant colony optimization." In *Proceedings of the first ACM/SIGEVO Genetic and Evolutionary Computation Summit*, Shanghai, China, ACM, (2009), pp.601-608.
- [16] V.S. Prajapat, A.R. Kyada, T.M. Patel, "Topology Optimization of Automotive Disc Brake using FEA-DOE Hybrid Modeling", *IOSR Journal of Mechanical and Civil Engineering (IOSR-JMCE)* e-ISSN: 2278-1684,p-ISSN: 2320-334X, Volume 14, (2017), pp.72-80.
- [17] A. Kaveh, B. Hassani, S. Shojaee, Sh.M. Tavakkoli. "Structural topology optimization using ant colony methodology." *Engineering Structures* 30, no. 9 (2008), pp.2559-2565.
- [18] Ch. Bastien, J. Christensen, M. Blundell, J. Kurakins. "Lightweight Body in White Design Using Topology-, Shapeand Size Optimisation." *World Electric Vehicle Journal* 5, no. 1 (2012), pp.137-148.
- [19] C.Fountzoulas, G. Gazonas, B. Cheeseman. "Computational modeling of tungsten carbide sphere impact and penetration into high-strength-low-alloy (HSLA)-100 steel targets." *Journal of Mechanics of Materials and Structures* 2, no. 10 (2007), pp.1965-1979.
- [20] D.R. Lesuer, G.J. Kay, M.M. LeBlanc. "Modeling large-strain, high-rate deformation in metals." No. UCRL-JC-134118. Lawrence Livermore National Lab., CA (US), (2001).
- [21] J. Marzbanrad, M. Mehdikhanlo, A. Saeedipour, ""An energy absorption comparison of square , circular , and elliptic steel and aluminum tubes under impact loading", *Turkish Journal of Engineering and Environmental Sciences*, vol. 33, (2009), pp.159-166.
- [22] B.A. Conway, "A survey of methods available for the numerical optimization of continuous dynamic systems." *Journal of Optimization Theory and Applications* 152, no. 2 (2012), pp.271-306.
- [23] C. Kane, M. Schoenauer. "Topological optimum design using genetic algorithms." *Control and Cybernetics* 25 (1996), pp.1059-1088.
- [24] M.A. Ochoa Montes, "Topology optimization algorithms for the solution of compliance and volume problems in 2D" M.Sc. Thesis, Centro de Investigación en Matemáticas, Guanajuato, Mexico, (2016).
- [25] M. Afrousheh, J. Marzbanrad, D. Göhlich. "Topology optimization of energy absorbers under crashworthiness using modified hybrid cellular automata (MHCA) algorithm." *Structural and Multidisciplinary Optimization* (2019), pp.1-14.

- [26] S. Khan, M. Abd-El-Barr. "A Hybrid Ant Colony Optimization Algorithm for Topology Optimization of Local Area Networks." In 2018 International Conference on Computing Sciences and Engineering (ICCSE), Kuwait, IEEE, (2018), pp.1-5.
- [27] K. S. Yoo, S.Y. Han. "Modified ant colony optimization for topology optimization of geometrically nonlinear structures." International journal of precision engineering and manufacturing 15, no. 4 (2014), pp.679-687.